frontiers | Frontiers in Energy Research

TYPE Original Research
PUBLISHED 26 January 2023
DOI 10.3389/fenrg.2023.1120108

OPEN ACCESS

EDITED BY
Chuangchuang,
Massachusetts Institute of Technology,
United States

REVIEWED BY
Jun Li,
Guangzhou Institute of Energy Conversion (CAS), China
Bo Jiang,
Nanjing University of Science and Technology, China

*CORRESPONDENCE
Mingming Huang,
dahuangby@sina.com

SPECIALTY SECTION
This article was submitted to Advanced Clean Fuel Technologies, a section of the journal Frontiers in Energy Research

RECEIVED 09 December 2022
ACCEPTED 18 January 2023
PUBLISHED 26 January 2023

CITATION
Zhang Y, Zhao D, Li Q, Huang M, Hao Q, Du J, Song Y, Ming Z and Wang J (2023), Premixed combustion and emission characteristics of methane diluted with ammonia under F-class gas turbine relevant operating condition. *Front. Energy Res.* 11:1120108. doi: 10.3389/fenrg.2023.1120108

Premixed combustion and emission characteristics of methane diluted with ammonia under F-class gas turbine relevant operating condition

Yanfei Zhang[1,2], Dapeng Zhao[1,2], Qin Li[3], Mingming Huang[1,2]*, Qing Hao[1], Jianji Du[4], Yang Song[1,2], Zhaoqing Ming[1,2] and Jihang Wang[1,2]

[1]School of Mechanical Engineering, Qilu University of Technology (Shandong Academy of Sciences), Jinan, China, [2]Shandong Institute of Mechanical Design and Research, Jinan, China, [3]School of Material Science and Engineering, Qilu University of Technology (Shandong Academy of Sciences), Jinan, China, [4]Shandong Torch Creation Energy Science and Technology Co., Ltd., Jinan, China

Ammonia has been used on a small scale in other industrial equipment, such as gas turbines, as a carbon-free fuel. However, ammonia fuel suffers disadvantages such as high ignition temperature, low flame velocity and high NO_x emissions. Doping with ammonia using a more reactive fuel, such as methane, can solve the above problems. Therefore, under the relevant operating conditions of the gas turbine (T = 723 K, p = 16.5 atm), the effect of ammonia content on the combustion and emission characteristics of laminar premixed methane flames was numerically investigated. This research uses the PREMIX code from ANSYS CHEMKIN-PRO 2020 and Okafor chemical kinetic mechanisms and provides a reference for our subsequent analysis of gas turbine operating conditions. Firstly, the emission data of major pollutants under different ammonia content (X_{NH3} = 0–1.0) and equivalent ratio (Φ = .6–1.4) were calculated. Then, the laminar premixed flame structure is analyzed under the lean fuel conditions associated with gas turbines (Φ = .6, .8). Finally, the effect of ammonia addition on the chemical reaction path of NO and CO emission was studied. The results show that ammonia/methane mixture fuel is more suitable for combustion at $.6 < \Phi < .8$ under high temperature and pressure. High ammonia content ($X_{NH3} > .6$) and low equivalent ratio can reduce NO and CO emissions. The molar fractions of H, O, and OH radicals and flame temperature decreased with the increase in ammonia content. In addition, high temperature and high pressure conditions and ammonia content greatly influence the reaction path of NO and CO production. The increase in pressure resulted in a change in the primary reaction that produced NO. In conclusion, this study guides reducing the emission of NO and CO from lean side of gas turbine plants.

KEYWORDS

ammonia combustion, gas turbine, NO emission, carbon neutrality, carbon emission

1 Introduction

To address the shortage of fossil fuels and global warming, using carbon-free sustainable fuels in industrial equipment such as gas turbines is a practical approach (Michailos and Gibbins, 2022). Using ammonia fuel will significantly reduce greenhouse gas (such as carbon dioxide) emissions as it is carbon-free. As a sustainable chemical energy, ammonia can be

synthesized from fossil fuels, biomass, or other renewable sources such as solar, wind, geothermal, and biomass (Zamfirescu and Dincer, 2008). The carbon dioxide produced during the synthesis can be captured, resulting in ammonia production with a shallow carbon footprint (Kobayashi et al., 2019). Compared with hydrogen, ammonia can be liquefied at room temperature and a pressure of 8.5 bar, so the storage and transportation of ammonia fuel are much easier (Collis and Schomäcker, 2022; He et al., 2022).

As a hydrogen carrier fuel, the application of ammonia in gas turbines has been realized (Valera-Medina et al., 2017; Berwal et al., 2021). For example, NH_3–air combustion power generation has been successfully realized using a 50 kW class micro gas turbine system (Kurata et al., 2017). Although ammonia can replace hydrocarbon fuel in gas turbines, the consumption of ammonia fuel is 2.25 times higher than that of methane fuel for the same power output. In addition, ammonia fuel has the disadvantages of low laminar flame velocity, narrow flammability equivalence ratio, and high minimum ignition energy (Chen et al., 2022). These disadvantages result in a flame that isn't easily ignited, has poor stability, and has a low heat release rate. Due to the presence of the N element in NH_3 molecules, the problem of high NO_x emission caused by ammonia fuel needs to be solved. In order to improve the characteristics of ammonia, more reactive fuels can be used for doping with ammonia, such as methane (Valera-Medina et al., 2015) and hydrogen (Zhang et al., 2022). Since methane is the main component of natural gas fuel widely used in gas turbines, using ammonia/methane blends is one way to promote ammonia as an alternative fuel to natural gas (An et al., 2021; Sun J. et al., 2022). To design an advanced gas turbine combustor, the ammonia/methane fuel in the combustor must achieve the goal of stable combustion and low NO_x emission. Therefore, it is necessary to study the combustion characteristics of the ammonia/methane mixture, such as combustion speed, flame temperature, and NO_x emission.

Several researchers have explored the potential combustion properties and chemical mechanism studies of ammonia/methane mixtures at ambient temperature and pressure (Khateeb et al., 2020; Colson et al., 2021; Xiao et al., 2020; Nozari and Karabeyoğlu, 2015). For example., Jójka and Ślefarski. (2018) conducted experimental and numerical studies on the combustion process of ammonia-doped methane flames with ammonia content ranging from 1% to 5% (volume fraction). The results showed that nitrogen oxide emissions increased with increasing ammonia content, but the increasing trend wasn't linear. Increasing the ammonia content in the fuel from 2.5% to 5% by volume only increased the NO emissions of the mixture by 55.5% (from 946 ppmv to 1,471 ppmv). Ku et al. (2020) studied the combustion characteristics of premixed ammonia/methane air flame. The results show that the premixed ammonia/methane flame is thicker and propagates slower than the pure methane flame. When the ammonia level was increased from 20% to 40%, the data showed a 25% reduction in CO_2 emissions; Kovaleva et al. (2022) studied the exhaust gas content of laminar premixed ammonia/methane flames at two ammonia contents (20% and 60% by volume). Sensitivity and reaction path analyses were performed on the Okafor mechanism, and reaction rate constants were improved. Finally, the performance of the N_2O component in the rich region is improved, highlighting the importance of the HNO + CO = NH + CO_2 reaction. Rocha et al. (2019) investigated the effect of different ammonia contents (30% and 80% volume fraction) on NO emissions from premixed ammonia/methane fuels. It is clearly stated in the paper that the formation of most NO at normal temperature and pressure is determined by the reactions of HNO + OH = NO + H_2O and HNO + H=NO + H_2 during the combustion process. The above numerical analysis or experiments are all carried out under normal temperature and pressure conditions. Still, research under high temperature and high pressure conditions is the current development direction because high temperature and high pressure represent practical industrial conditions (such as gas turbines).

There are few studies on the combustion characteristics of ammonia/methane blends under practical gas turbine conditions. Under the condition of high temperature and high pressure, grasping the effect of increasing ammonia content on the combustion characteristics of methane has a propelling effect on accelerating the application of ammonia/methane blends in gas turbines. Okafor et al. (2019) measured the non-extensional laminar burning velocity and Markstein length of an ammonia/methane flame (ammonia heat fractions in the fuel ranging from 0 to .3) at room temperature and high pressure (0.1–.50 MPa), and proposed an optimized Okafor reaction mechanism. The results show that the accurate prediction of laminar combustion velocity and NO concentration in ammonia-containing flames may depend on the accuracy of the prediction of O/H radical concentration. Khateeb et al. (2021) studied the stability limits and NO emissions of premixed ammonia/methane flames. Experiments were carried out at room temperature and pressure of 1–5 bar. The results show that the broadest range of the stable equivalence ratio of X_{NH3} = .8 fuel is .7 at 5 bar. The variation of the stability limit with pressure is attributed to the increase in the Reynolds number; Berwal et al. (2023) measured the laminar combustion velocity of different CH_4/H_2/NH_3 mixture concentrations at a higher mixture temperature (300–750 K) and atmospheric pressure. In a 4:1 ratio of CH_4:H_2 fuel mixture, the volume fraction of ammonia varies from 0% to 30%. Sensitivity analysis showed that H + O_2 = O + OH and OH + CO = H + CO_2 were the most important in improving the combustion rate of the mixture. The reaction pathway diagram explains the different oxidation features in the laminar burning velocity (LBV) increment and the reduction of ammonia in the current composition, where the increase in HCO to H leads to the consumption of H radicals by HNO to form NO. Xiao et al. (2017b) studied the effect of high pressure and (1–20 atm) and temperature (400–800 K) on a 60% ammonia/40% methane fuel mixture. The study shows that at an initial temperature of 800 K, the laminar flame velocity of ammonia/methane blends decreases significantly with increasing pressure. As the pressure increased, both CO and NO emissions decreased. The above literature shows that most of the research based on ammonia/methane mixed fuel is carried out under a small range of heating or pressurization, There are few reports on the comprehensive study of combustion and emission characteristics under the combined effect of temperature and pressure. Especially in the gas turbine operating condition (T = 723 K, p = 16.5 atm), there are still many places that need to be clarified about the dominant reaction and mechanism of NO generation. The F-class gas turbine is a type of internal combustion engine, and the compression process of its compressor will cause the initial temperature of the unburned ammonia/methane mixture to rise to about 723 K. The initial pressure rises to 16.5 atm, usually operating under lean burn conditions (Sun Y. et al., 2022). The reduction mechanism of ammonia/methane combustion under practical gas turbine combustor conditions were explored (Xiao et al., 2017a). In order to meet the gas turbine combustor conditions, the inlet temperature was set to 600 K, and the pressure

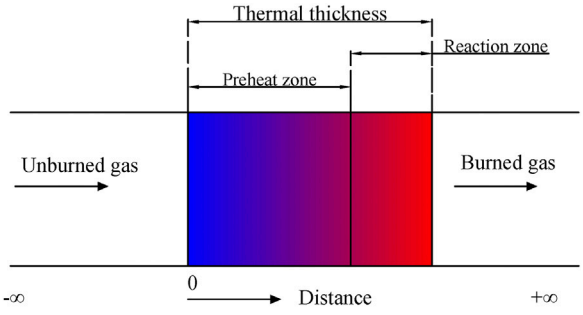

FIGURE 1
Schematic illustration of a laminar premixed flame.

was 17 atm. Therefore, the initial temperature of 723 K and the initial pressure of 16.5 atm can represent typical gas turbine operating conditions. In addition, most of the previous related work only studied the partial addition of ammonia to methane. At the same time, this paper comprehensively analyzes the combustion characteristics of different ammonia content (X_{NH3} = 0–1.0) in ammonia/methane fuel. Previous studies on the emission characteristics of the ammonia/methane combustion process mainly focus on NO_x emissions, and the research on CO emissions is still limited. Insufficient combustion of methane tends to produce CO, which leads to lower combustion efficiency. Therefore, it is also of great significance to study the effect of ammonia content on CO emissions.

This paper mainly studies the effect of ammonia addition on methane combustion and NO and CO emission characteristics through numerical simulation with chemical reaction mechanism under the condition of gas turbine heating and pressurization (T = 723 K, p = 16.5 atm). T = 723 K, p = 16.5 atm can provide a reference for studying gas turbine-related high preheat and high pressure conditions. First, The change of primary pollutant emission with equivalent ratio (Φ = .6–1.4) under different ammonia content was studied. Since radicals (H, O, OH, and NH_2) and flame temperature affect the amount of LBV and NO generated, this paper discusses the effect of increasing ammonia content on these important radicals and combustion temperature. Unlike pure methane or hydrogen, most NO_x emissions from ammonia fuels are formed through the fuel NO_x pathway. In order to reduce NO_x emissions below acceptable values, NO_x emissions can be reduced by operating lean (Φ < 1) (Glarborg et al., 2018) or rich (Φ > 1) (Okafor et al., 2020). However, rich combustion isn't conducive to the improvement of gas turbine performance, and unburned ammonia emissions are also harmful to the environment. In addition, high-preheat environments can lead to high NO_x formation through the thermal NO_x path. Therefore, at the end of this paper, the effect of adding ammonia on NO and CO emissions was studied under the gas turbine-related lean-burn conditions (Φ = .6, .8). Among them, an equivalence ratio of .6 represents the lean limit of pure ammonia fuel (Valera-Medina et al., 2018). In conclusion, this study will enrich the ammonia combustion database and provide new guidance for designing low-carbon and high-efficiency ammonia-fueled gas turbines.

2 Models and validation

2.1 Computational models

The 1D free-propagating PREMIX flame model on Chemkin-PRO 2020 was used to analyze the oxidation chemistry of the mixture and 1D simulations. Figure 1 shows the flame model of the combustion process. The laminar premixed flame layer is divided into preheating and reaction zones during the combustion process. The preheat zone is formed by the continuous heating of the mixture in a laminar premixed flame layer. The "distance" here refers to the laminar premixed flame propagation distance.

During the calculation, the initial value of the mass flow rates was adjusted to the same thermal input (1200 W). The tested cases are shown in Table 1. The distance of the computational domain varies from 0 to .3 cm. The mesh refinement criteria are set to GRAD = .1 and CURV = .2. The total number of meshes generated is about 2,000, and the adaptive mesh is 500. In the iteration process, the relative and absolute errors are set at 10^{-4} and 10^{-9}. The initial temperature and pressure for the simulation were 723 K and 16.5 atm unless explicitly stated otherwise. When the initial temperature was set to T = 723 K, the fixed temperature was set to 800 K. The convection term was discretized using the upwind difference scheme, and the diffusion coefficient of the mixture was calculated using the averaging method. In addition, the Soret effect was considered in all studied operating conditions. Φ was set to .6 and .8.

The laminar burning velocity of an ammonia/methane blended flames is defined as

$$S_L = \left[2\left(\frac{D_T}{\omega_{f,u}\rho_u}\right)\overline{RR}\right]^{1/2} \tag{1}$$

Where D_T is the thermal diffusion coefficient, $\overline{RR}$ represents the average reaction rate of the mixed gas in the reaction zone, ρ_u represents the density of unburned gas, and $\omega_{f,u}$ is the mass fraction of the unburned fuel.

The following equations can be used to express the change in laminar combustion velocity for ammonia/methane blended fuel at different temperatures and pressures.

$$S_L = S_{L,0}\cdot\left(\frac{T_i}{T_{i,0}}\right)^{\alpha}\cdot\left(\frac{P_i}{P_{i,0}}\right)^{\beta};\ \alpha = 1.81 + 0.058\cdot\frac{P_u}{P_{u,o}};\quad \beta = 0.098\cdot\frac{T_u}{T_{u,o}} - 0.4689 \tag{2}$$

where $S_{L,0}$ is the unstretched laminar burning velocity under reference conditions, α is the temperature exponent, β is the pressure exponent, $T_{i,0}$ and $P_{i,0}$ are the reference temperature and pressure. Reference conditions depend on the temperature and pressure conditions to be analyzed.

The reaction rate of chemical reaction and the formation rate of components can be calculated by using the reaction rate constant. The positive chemical reaction rate constant k is calculated by the Arrhenius equation:

$$k = AT^b \exp\frac{-E_a}{RT} \tag{3}$$

The chemical reaction rate of a substance is

10.3389/fenrg.2023.1120108

TABLE 1 Flame conditions for ammonia/methane blended fuel.

Number	Equivalence ratio (Φ)	Fuel component (volume)		Fuel flow rate (g/s)	Air flow rate (g/s)
		CH_4	NH_3		
1	0.6	100	0	0.024	0.702
2		80	20	0.027	0.689
3		60	40	0.032	0.673
4		40	60	0.037	0.651
5		20	80	0.045	0.621
6		0	100	0.056	0.577
7	0.8	100	0	0.024	0.516
8		80	20	0.027	0.507
9		60	40	0.032	0.495
10		40	60	0.037	0.479
11		20	80	0.045	0.457
12		0	100	0.056	0.424

TABLE 2 Three mechanisms used in the current work.

Mechanism	Species	Reactions	Ref
GRI Mech 3.0	53	325	Ren et al. (2019)
San Diego	111	784	Mikulčić et al. (2021)
Okafor	59	356	Okafor et al. (2018)

$$RR_{xi} = k\left[\frac{P}{RT}\right]^{n-1}[x_i]^n \tag{4}$$

Where k is the reaction rate constant at temperature T, A is the frequency factor or Arrhenius constant, E_a is the reaction activation energy, T is the absolute temperature, R is the ideal gas constant, P is the reaction pressure, and x_i is the relative concentration change rate (mole fraction).Where X_{NH3} is the volume fraction of NH_3 in the fuel mixture, The ammonia fuel fraction is adjusted by changing the ratio of the volume flow of ammonia V_{NH3} to the volume flow of methane V_{CH4}. The ammonia fuel volume fraction value is defined as:

$$X_{NH3} = \frac{V_{NH3}}{V_{NH3} + V_{CH4}} \tag{5}$$

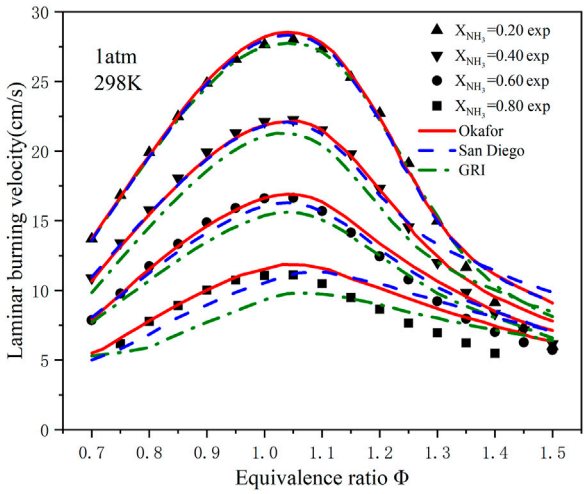

FIGURE 2
Experimental and simulated LBVs at T = 298 K, p = 1 atm. (Symbols: experimental data; lines: Simulated data).

Validation of the computational model

In order to accurately predict the flame characteristics and NO, CO emissions of ammonia/methane blended fuel, we need a reaction mechanism that can satisfactorily simulate the laminar burning velocity (LBV). Therefore, three widely accepted and used chemical kinetic mechanisms were selected. Table 2 provides details of the three mechanisms.

Figure 2 shows the LBV of ammonia/methane blended fuel flames with different ammonia contents (X_{NH3} = .2–.8) at room temperature and pressure. To verify the accuracy of the selected chemical kinetic mechanisms, Figure 2 compares the calculated LBV values for the three mechanisms with experimental data in related literature (Han et al., 2019). As seen from the Figure 2, compared with the other two mechanisms, the predicted value of the GRI mechanism is quite different from the experimental results. However, within the equivalence ratio range of .7–1.05, the predicted value of the GRI mechanism is still accurate. The comparison with the experimental results shows that the predicted value of the Okafor mechanism is the most precise on the lean side, and the predicted value and the experimental data have been very overlapped. Furthermore, these three mechanisms perform well with X_{NH3} = .2. As the ammonia content increased, the San and GRI mechanisms no longer fit the

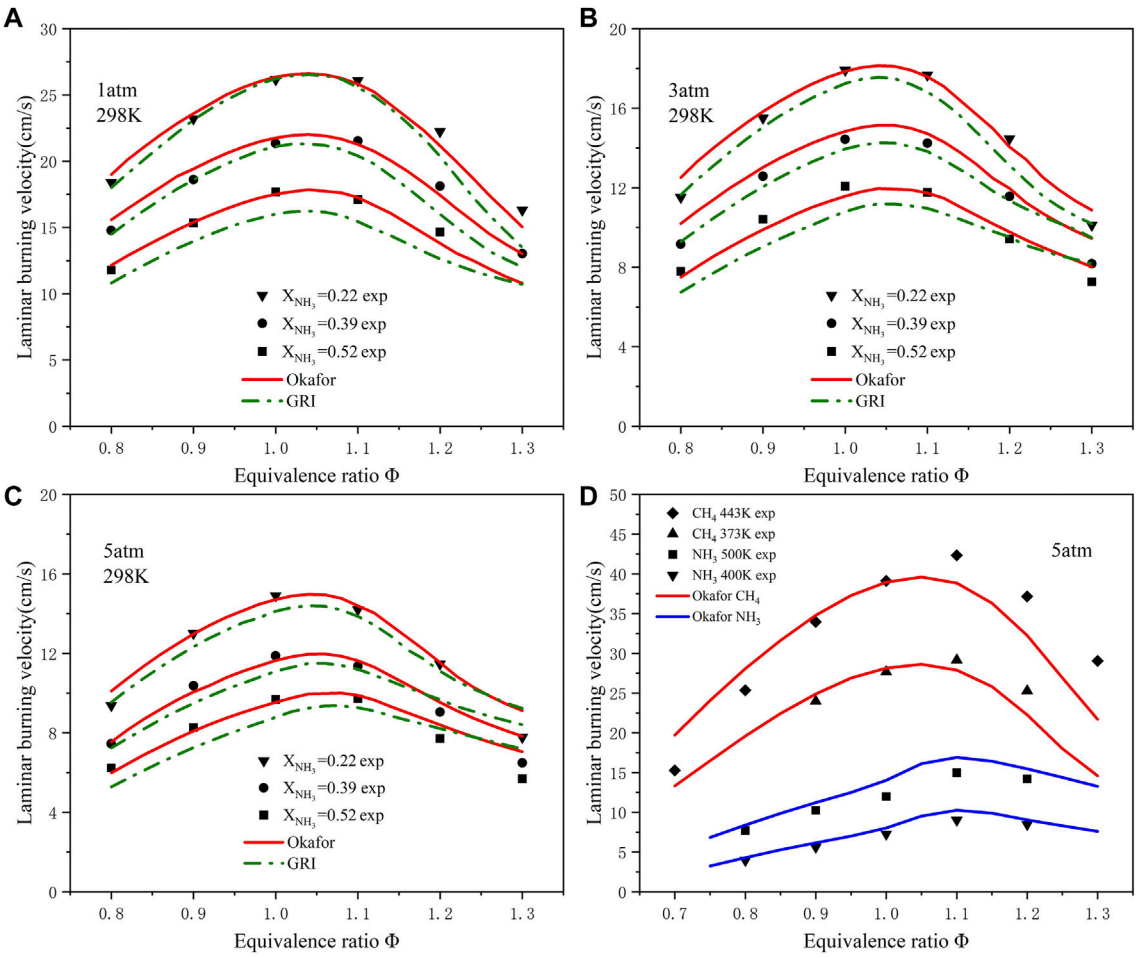

FIGURE 3
Comparison of experimental and simulated LBVs at different pressures and initial temperatures: **(A)** T = 298 K, p = 1 atm; **(B)** T = 298 K, p = 3 atm; **(C)** T = 298 K, p = 5 atm; **(D)** When p = 5 atm, comparison of experimental and simulated LBVs of ammonia and methane at different initial temperatures. (Symbols: experimental data; lines: Simulated data).

experimental data. Under high ammonia contents combustion conditions, only the Okafor mechanism is more suitable for ammonia/methane combustion.

In order to study the combustion of ammonia/methane mixed fuel under gas turbine conditions, Figures 3A–C and compare the predicted values of each component of mixed ammonia fuel at room temperature and different pressures with the previous experimental data (Okafor et al., 2019). The results show that the Okafor mechanism still meets the experimental criteria under pressurized conditions, while the laminar flame velocity under the GRI mechanism is slightly lower than the experimental data. In addition, in the experimental environment of 5 atm, the temperature increase verification of pure methane and pure ammonia fuel was carried out, respectively. The results are in Figure 3D shows that the data predicted by the Okafor mechanism fit the experimental data very well (Hu et al., 2015; Kanoshima et al., 2022), so the Okafor mechanism was selected among the three mechanisms. The characteristics of pollutant emission in ammonia combustion were studied under high temperature and high pressure (T = 800 K and p = 20 atm) using the Okafor mechanism (Cheng et al., 2021). Therefore, the research conducted in this paper under the operating conditions of an F-class gas turbine (T = 723 K and p = 16.5 atm) can ensure the accuracy of the Okafor mechanism.

3 Results and discussion

3.1 LBV and NO and CO emissions under different initial temperatures and pressures

The study of laminar premixed combustion with T = 723 K and p = 16.5 atm helps to understand the effect of initial parameters on laminar premixed combustion. It is of great significance to study the effect of ammonia content on the combustion and emission characteristics of methane under relevant conditions of gas turbines.

Figure 4 shows the variation of LBV, NO, and CO emissions with X_{NH3} for different initial temperatures and pressures. From the overall trend, the LBV and CO emission decreased with the increase of ammonia content. With the increase of ammonia content, NO emission first increased and then decreased. When p = 1 atm, the emissions of LBV, NO, and CO increased with the initial temperature (T = 298–723 K). This is because the enthalpy of the reactant mixture

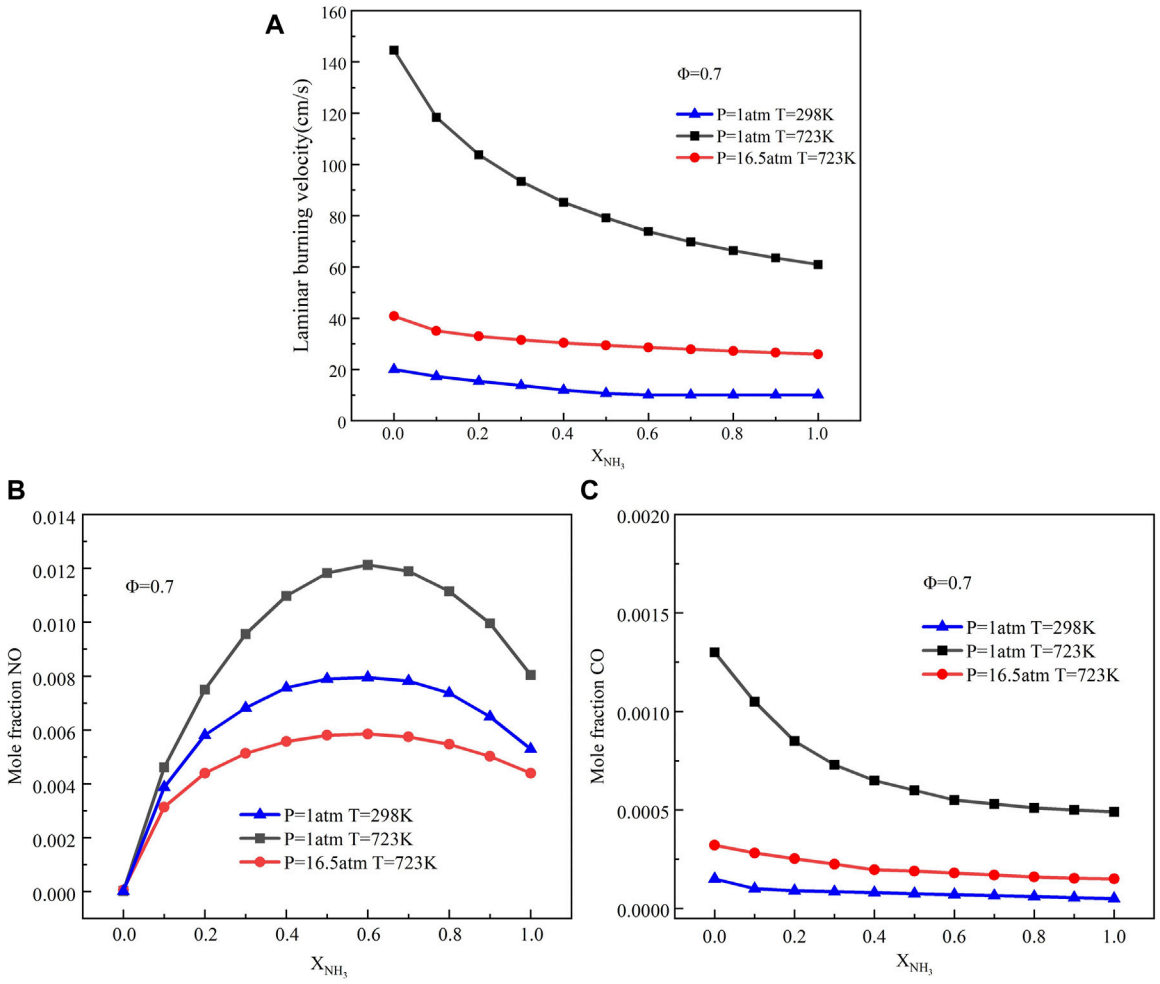

FIGURE 4
Variations of LBV, NO, and CO with ammonia content at different initial temperatures and initial pressures: **(A)** LBV; **(B)** NO emission; **(C)** CO emission.

increases with the initial temperature, and an increase in the enthalpy of the reactant mixture leads to an increase in the rate of combustion. In addition, Eq. 3 also shows that the reaction rate is exponentially related to temperature. An increase in the initial temperature of the combustible mixture can significantly promote the reaction rate, increasing LBV. The NO emission in ammonia/methane mixed flame is partly formed through the thermal NO pathway. The reaction rate of the thermal NO pathway is enhanced with the initial temperature increase, increasing NO emission. In addition, the dissociation reaction of carbon dioxide at high temperatures leads to an increase in CO production.

Then, it can be observed that when T = 723 K, the increase of pressure (p = 1.0–16.5 atm) leads to the decrease of LBV, NO, and CO emissions. The increase in pressure causes the density of the mixture to increase. Increasing mixture density reduces the mean free path of molecular collision and increases the collision frequency. This leads to enhanced third-body effects and higher third-body recombination reactions. Thus, the decrease in LBV was attributed to an enhanced third-body recombination reaction and increased density (Varghese et al., 2019). The decrease of NO emissions with increasing pressure indicates that pressure is an important factor affecting the kinetics of fuel NO formation. Previous studies have shown that the effect of fuel NO is more significant than that of thermal NO in high pressure environments. In addition, O, H, and OH radicals are heavily depleted with increasing pressure, leading to a decrease in NO formation (Okafor et al., 2019). According to Eq. 4, the increase in initial pressure leads to a rapid increase in the reaction rate of combustion. Higher combustion rates result in less CO production. Interestingly, Under the condition of high temperature and pressure, the emission level of NO is lower than that of normal temperature and pressure. In addition, CO emissions at high temperatures and pressure are very close to those at room temperature and pressure. Therefore, increasing pressure is a good way to solve the problem of NO emissions.

3.2 Effect of equivalence ratio on emission of major pollutants

The research in the previous section shows that the NO and CO emissions of the ammonia/methane mixed fuel show a strong dependence on the initial temperature and pressure. Under the working condition of a gas turbine (T = 723 K, p = 16.5 atm), it is of great significance to study the influence of the equivalence ratio on

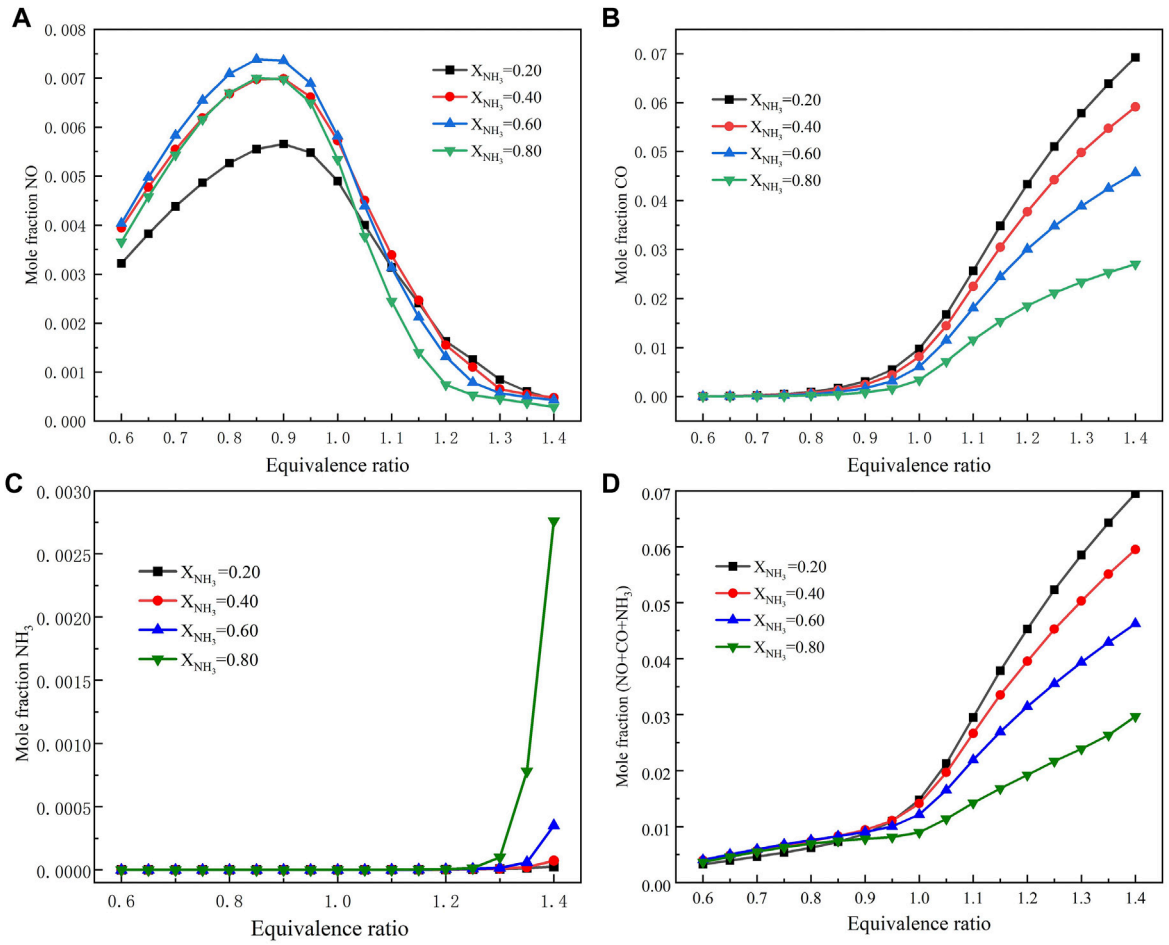

FIGURE 5
Emission of major pollutants as a function of equivalent ratio: **(A)** NO emission; **(B)** CO emission; **(C)** NH_3 emission; **(D)** Emission of total pollutants.

the emission of primary pollutants from ammonia/methane mixed fuel.

Figure 5 shows the numerical simulation results of the main emission pollutants (NO, CO, and NH_3) after the combustion of ammonia/methane mixture fuel (X_{NH3} = .2–.8) at high temperature and pressure (T = 723 K, p = 16.5 atm). Figure 5A shows that the NO emission level of ammonia/methane mixed fuel increases with the increase of the equivalent ratio, reaches the maximum at Φ = .9, and finally decreases with the increase of the equivalent ratio. This is because there is a lot of unreacted ammonia in the fuel-air mixture at a high equivalence ratio. Ammonia participates in the reaction to produce a large amount of NH_2, and part of NO is removed by further reaction with NH_2; Figure 5B shows that with the increase of the equivalent ratio, CO emission shows an increasing trend. For .6 < Φ < .8, CO emissions barely grow. Then, when Φ > .8, the CO emission increases rapidly with the increase of the equivalent ratio; Figure 5C shows the same trend, with unburned NH_3 emission levels beginning to climb rapidly after Φ > 1.3. The increasing trend becomes less obvious when X_{NH3} < .2; Figure 5D adds together the emission levels of the three major pollutants. The results show that the sum of emissions of pollutants increases rapidly after Φ > .9. Under the condition of .6 < Φ < .9, the total pollutant emission level of ammonia/methane mixture fuel increases very slowly at any ammonia content. In addition, in order to reduce carbon dioxide emissions, high ammonia content fuels can be selected as far as possible. Finally, it is concluded that when the ammonia/methane mixture fuel is burned under single-stage premixed gas turbine conditions (T = 723 K, p = 16.5 atm), it is best to burn under fuel lean conditions.

In order to verify the above conclusions, the emission data of NO and CO in Figures 5A, B and at high temperature and pressure were compared with previous studies at normal temperatures and pressure (Xiao et al., 2017b). The results show that the peak NO emission level of various ammonia content fuels under T = 723 K and p = 16.5 atm is reduced by half compared with that under normal temperature and pressure conditions, while the CO emission is almost unchanged. This indicates that NO emission is more sensitive to pressure than CO, and pressure can reduce the NO emission level more. Although the emission level of NO is lower under the condition of fuel rich, the problem of high CO and NH_3 caused by fuel rich needs to be solved. The problem of high NO caused by fuel poor can be solved by increasing pressure. In conclusion, combustion under high pressure and fuel lean conditions is a good way to solve the emission problem of

10.3389/fenrg.2023.1120108

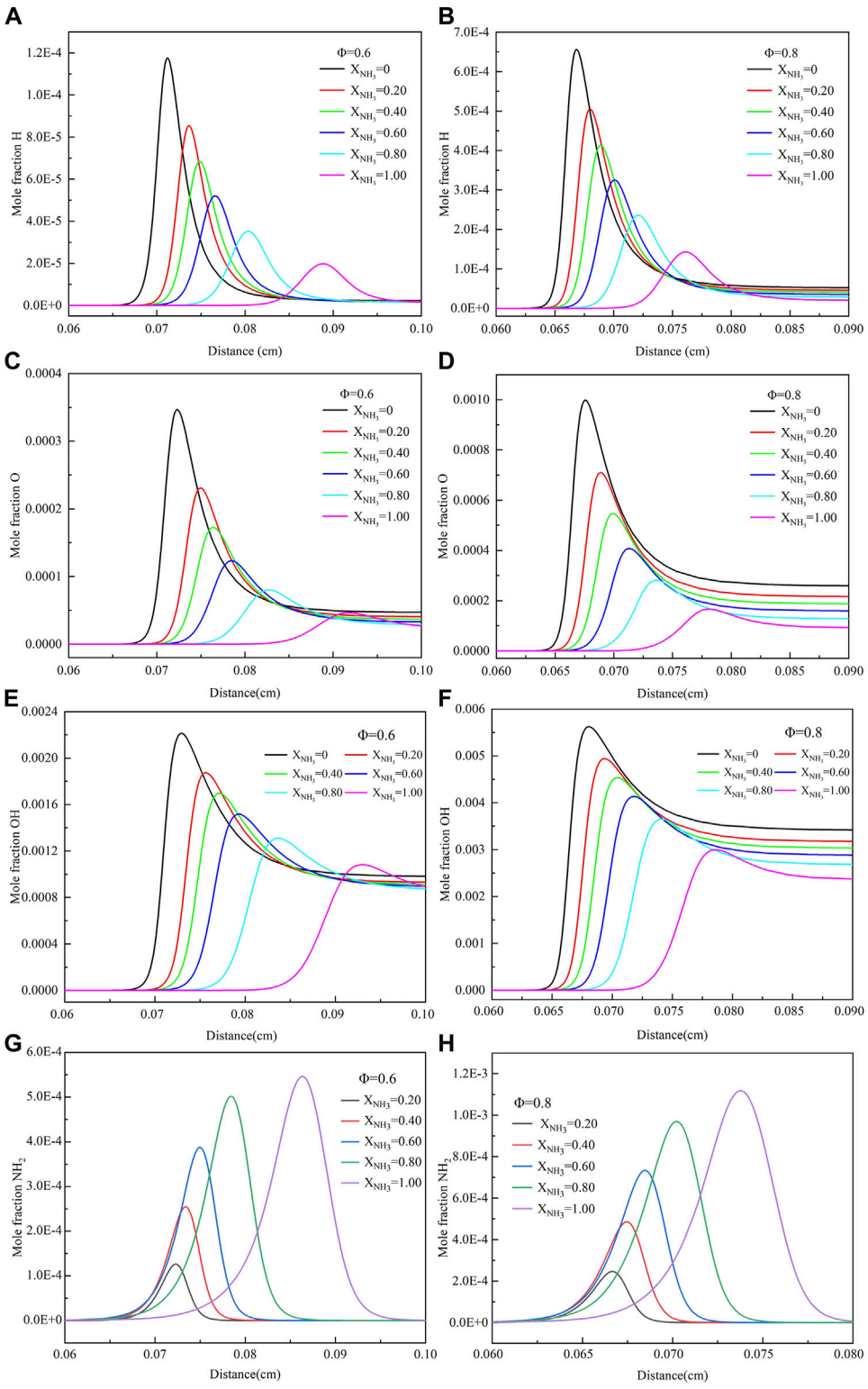

FIGURE 6
The mole fraction of H, O, OH, and NH_2 with different ammonia content: **(A)** When Φ = .6, the mole fraction of H; **(B)** When Φ = .8, the mole fraction of H; **(C)** When Φ = .6, the mole fraction of O; **(D)** When Φ = .8, the mole fraction of O; **(E)** When Φ = .6, the mole fraction of OH; **(F)** When Φ = .8, the mole fraction of OH; **(G)** When Φ = .6, the mole fraction of NH_2; **(H)** When Φ = .8, the mole fraction of NH_2. (T = 723 K, p = 16.5 atm).

ammonia/methane mixture fuel in a single-stage combustion system. Previous experimental (Kobayashi et al., 2019) studies have shown that the extinction limit of ammonia flames at high pressures increases significantly. Therefore, ammonia/methane fuel mixtures can be operated at lower equivalent ratios under gas turbine conditions (T = 723 K, p = 16.5 atm).

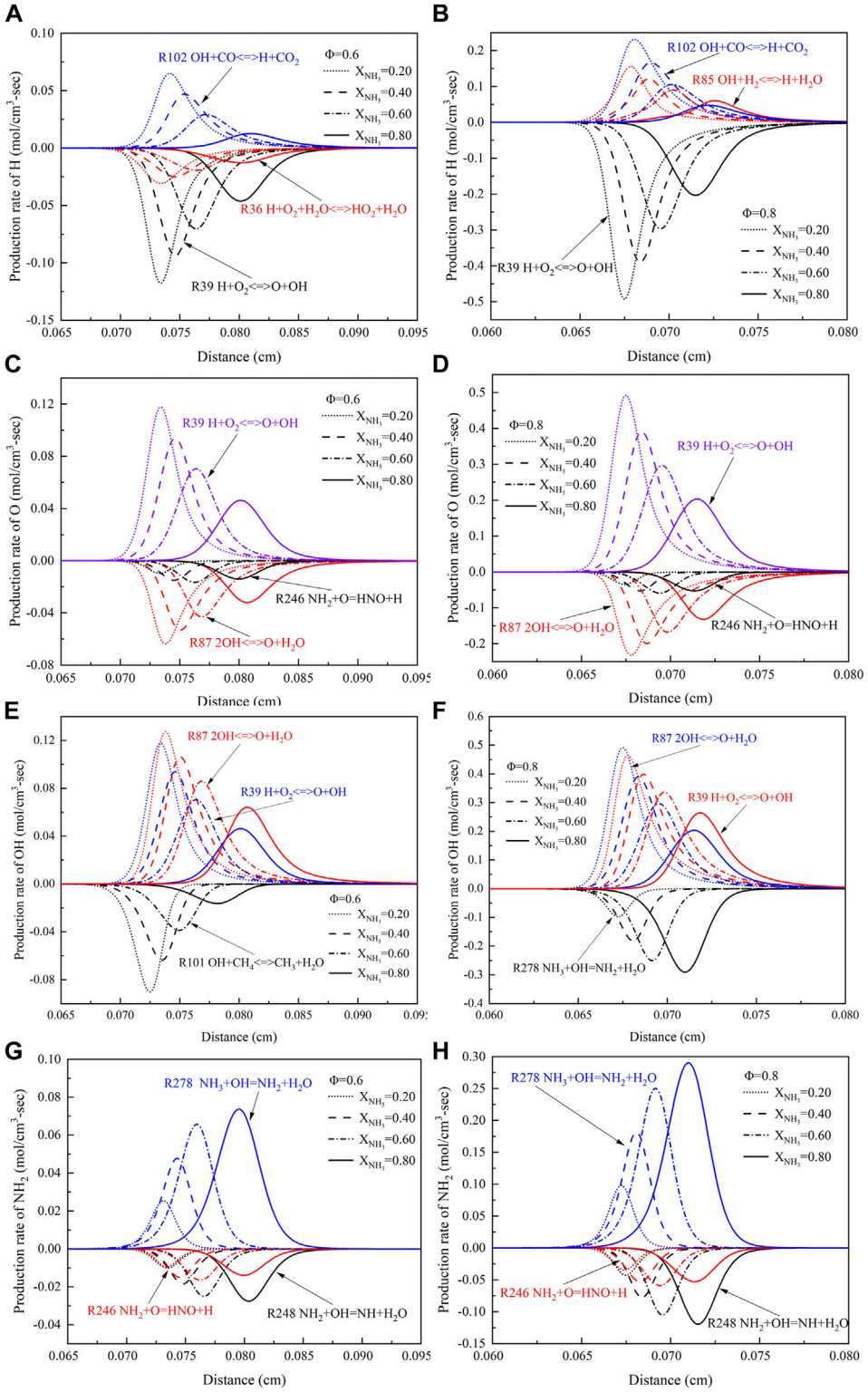

FIGURE 7
The generation rate of H, O, OH, and NH_2 with different ammonia content: **(A)** When Φ = .6, the generation rate of H; **(B)** When Φ = .8, the generation rate of H; **(C)** When Φ = .6, the generation rate of O; **(D)** When Φ = .8, the generation rate of O; **(E)** When Φ = .6, the generation rate of OH; **(F)** When Φ = .8, the generation rate of OH; **(G)** When Φ = .6, the generation rate of NH_2; **(H)** When Φ = .8, the generation rate of NH_2. (T = 723 K, p = 16.5 atm).

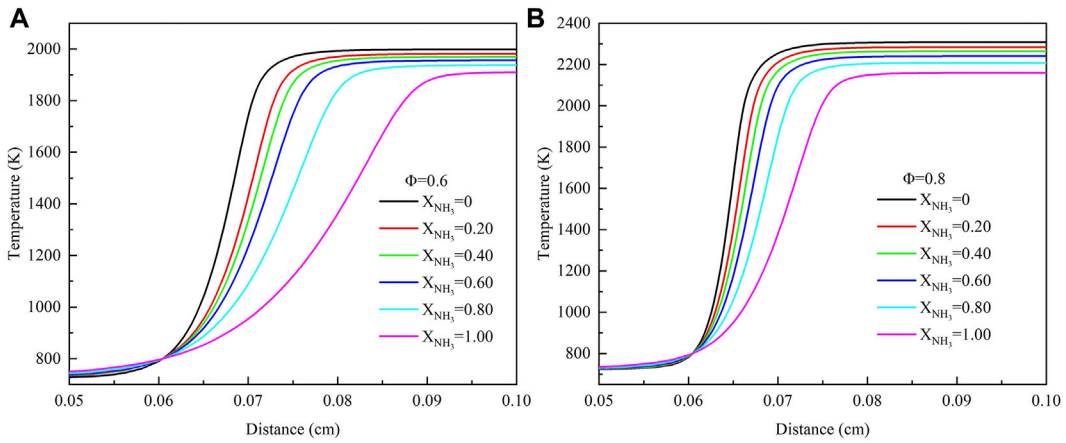

FIGURE 8
Mole fraction of temperature with different ammonia content: **(A)** Φ = .6; **(B)** Φ = .8. (T = 723 K, p = 16.5 atm).

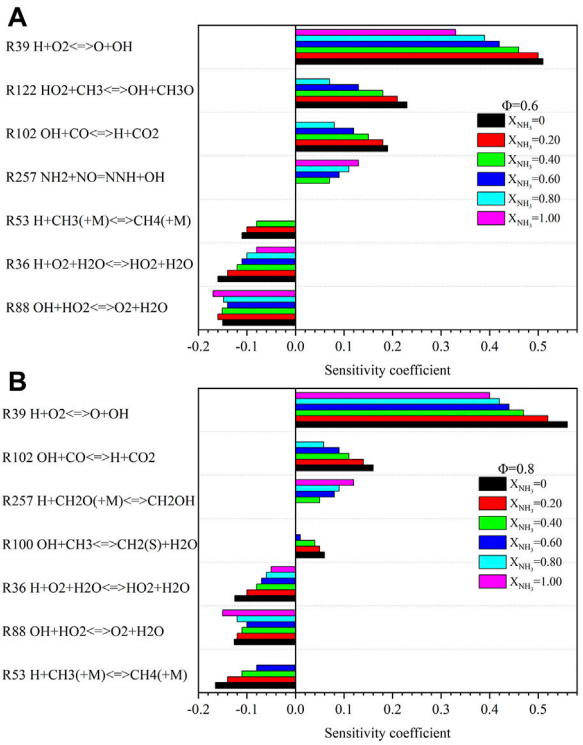

FIGURE 9
Sensitivity analysis of temperature with different ammonia content: **(A)** Φ = .6; **(B)** Φ = .8. (T = 723 K, p = 16.5 atm).

3.3 Effects of ammonia addition on H, O, and OH radicals

The analysis of free radical pools during combustion is very important for the study of combustion kinetics. Many studies have shown that flame propagation and laminar burning velocity are related to the production and consumption of OH, O, and H radicals in the flame. Furthermore, NH_2 radicals from ammonia start to appear after more ammonia replaces methane (Ren et al., 2019). The oxidation rate and reaction products of ammonia are highly dependent on the fate of NH_2 (Song et al., 2016). Therefore, the study of free radicals H, O, OH, and NH_2 contributes to understanding the flame chemical reaction kinetics of ammonia/methane mixtures and the entire combustion process.

Figure 6 shows the effect of X_{NH3} on the mole fractions of H, O, OH, and NH_2 under gas turbine conditions. It can be clearly observed that with the increase of X_{NH3} (X_{NH3} = 0–1.0) in the mixed fuel, the peak concentrations of H, O, and OH radicals gradually decrease. When the equivalent ratio is .8, the peak molar fraction of H radical is reduced by 76%, O by 82%, and OH by 47%. However, With the increase of X_{NH3} (X_{NH3} = .2–1.0), the peak molar fraction of NH_2 increased by 78%. The above results are because ammonia is relatively less reactive and has a lower flame temperature than methane. The increase in X_{NH3} also causes these radicals to form later. Under the two kinds of equivalent ratios, the molar fractions of H and O radicals decayed much faster after reaching their peaks than OH radicals. In addition, when the equivalence ratio increased from .6 to .8, the contents of free radicals H, O, OH, and NH_2 increased significantly. Compared with the free radical distribution under normal temperature and pressure conditions, the radical generation region under high temperature and high pressure are narrower, which has a great relationship with the increase in pressure.

To gain a deeper understanding of the flame structure of the ammonia/methane mixture, Figure 7 shows the effect of ammonia content (X_{NH3} = 0–1.0) on the H, O, OH, and NH_2 radical production rate at high temperatures and high pressure. The reactions shown in the Figure 7 are all essential reactions that generate or consume these free radicals. It can be seen that the main reactions to form H, O, and OH at two equivalent ratios are:

$$(R102)\ OH + CO <=> H + CO_2$$
$$(R39)\ H + O_2 <=> O + OH$$
$$(R87)\ 2OH <=> O + H_2O$$

The main reaction to form NH_2 is: (R278) $NH_3+OH = NH_2+H_2O$

The main reaction area of the combustion process is located where the peak concentrations of H, O, and OH radicals appear. The production rate of H, O, and OH radicals decreased significantly with the increase of X_{NH3}. In addition, the peak positions of H, O, and

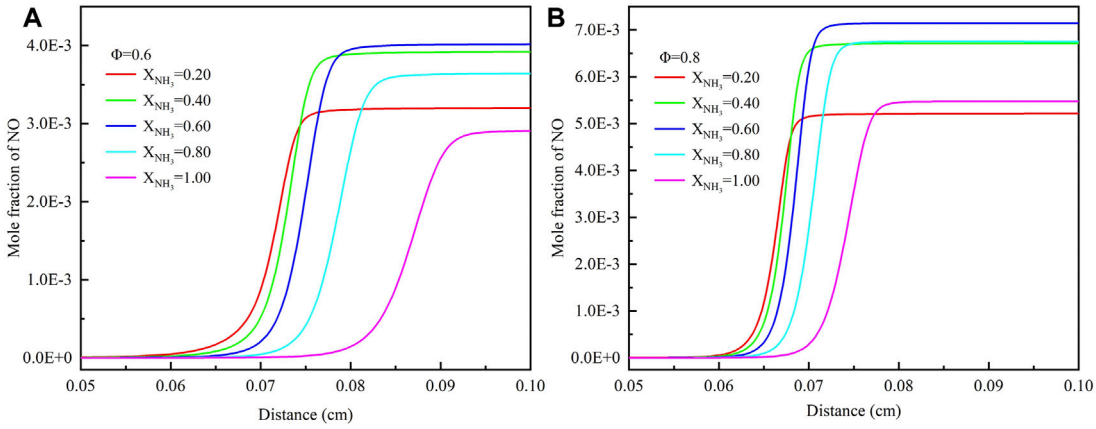

FIGURE 10
Mole fraction of NO with different ammonia content: **(A)** Φ = .6; **(B)** Φ = .8. (T = 723 K, p = 16.5 atm).

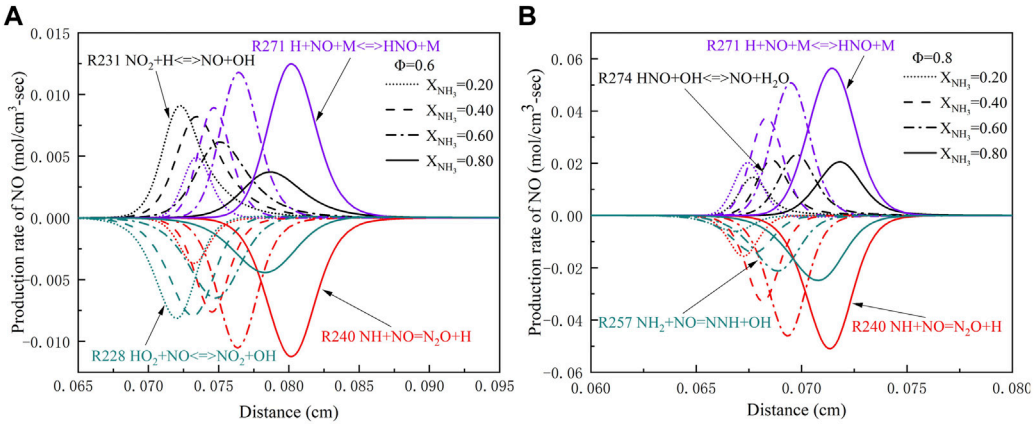

FIGURE 11
The production rate of NO with different ammonia content: **(A)** Φ = .6; **(B)** Φ = .8. (T = 723 K, p = 16.5 atm).

OH production rates shifted downstream with the addition of ammonia. Unlike H and O radicals, OH radicals are largely consumed with the increase of X_{NH3} at the equivalence ratio of 0.8. This shows that OH radicals play an important role in ammonia chemistry. In addition, NH_2 radicals affect NO production since a large amount of HNO and NH radicals are produced along with the consumption of NH_2.

3.4 Effects of ammonia addition on the temperature distribution

Figure 8 shows the effect of X_{NH3} on the flame temperature of ammonia/methane mixture combustion at high temperature and high pressure (T = 723 K, p = 16.5 atm). When X_{NH3} increased from 0 to 1.0, the reactivity of the mixture was reduced, resulting in a decrease in the flame temperature and an increase in the thickness of the reaction zone. In addition, the increase of X_{NH3} weakens the temperature gradient across the flame front region. The region where the temperature rises rapidly is about .06–.09 cm, also where the mole fractions of H, O, OH, and NH_2 radicals increase rapidly. Under normal temperature and pressure conditions, the region where the temperature rises rapidly and the region where the radical increases rapidly are about .05–.20 cm (Sun Y. et al., 2022). It is evident that an increase in pressure results in a reduction in the thickness of the reaction zone. Increasing the equivalence ratio from .6 to .8 can promote the combustion rate of the ammonia/methane mixture, resulting in a 300 K increase in the average flame temperature of the mixture.

Figure 9 shows the temperature sensitivity coefficients for Φ = .6 and .8 under high temperature and high pressure. For all the chain reactions, the four that contribute the most to the flame temperature can be identified.

$$(R39)\ H + O_2 < = > O + OH$$

10.3389/fenrg.2023.1120108

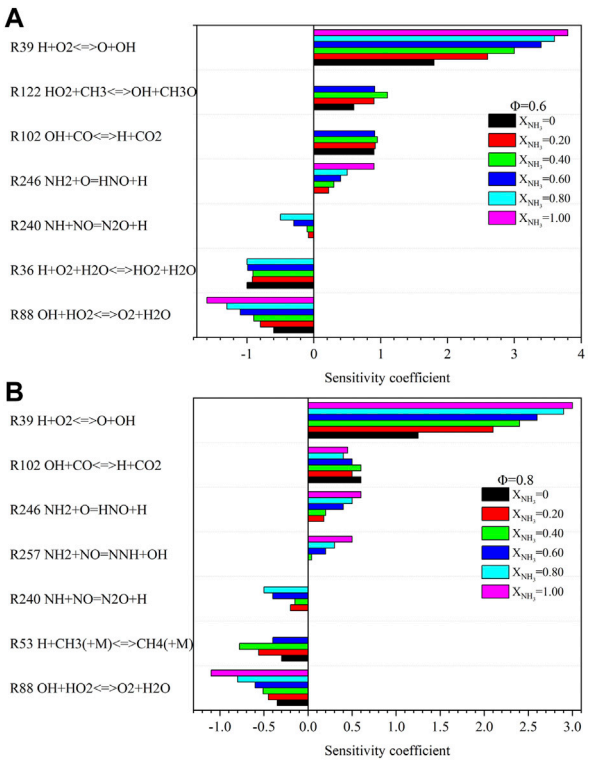

FIGURE 12
Sensitivity analysis of NO with different ammonia content: **(A)** Φ = .6; **(B)** Φ = .8. (T = 723 K, p = 16.5 atm).

$$(R102)\ OH + CO <=> H + CO_2$$
$$(R36)\ H + O_2 + H_2O <=> HO_2 + H_2O$$
$$(R53)\ H + CH_3(+M) <=> CH_4(+M)$$
$$(R88)\ OH + HO_2 <=> O_2 + H_2O$$

As an indicator of the overall burn rate, (R39) is the essential reaction that promotes temperature rise. It continuously produces high energetic radicals O and OH during the combustion process, which speeds up the chain reaction. As X_{NH3} increases from 0 to 1.0, the dominant effect of (R39) on temperature rise decreases. This is because the addition of ammonia content promotes the consumption of highly energetic radicals. The main reactions that suppress the flame temperature are (R88), (R53), and (R36). They consume OH and H radicals, respectively, and suppress the propagation of branched reactions. The enhanced three-body termination reaction (R53) under high pressure becomes less important with increasing ammonia content.

3.5 Effect of ammonia addition on NO formation

When ammonia is used as a fuel, NO_x emission issues need to be focused (Shi et al., 2022). Since the NO concentration in the product is much greater than that of NO_2 and N_2O, we focus on NO formation in the following analysis. Figure 10 shows the effect of ammonia addition (X_{NH3} = .2–1.0) on NO mole fraction under high temperature and high pressure environments. The results show that the equivalence ratio and ammonia content have significant effects on NO emissions from ammonia/methane blended fuels. Under lean fuel conditions, NO emission increases with the increase of equivalence ratio. Increasing the equivalence ratio from .6 to .8 resulted in a doubling of NO emissions. As can be seen from Figure 8, the reason for the above results is that with the increase of equivalence ratio, the flame temperature increases, and the increase of temperature leads to more NO formation through the thermal NO pathway. Besides, at both equivalence ratios, we can observe that NO emissions don't increase consistently with the increase of X_{NH3}. When X_{NH3} is greater than .6, NO emission decreases with the increase of X_{NH3}. This trend is the same as that under normal temperature and pressure conditions (Xiao et al., 2017b) and can also be observed in Figure 7; Figure 11.

As can be seen from Figure 7H, with the increase of X_{NH3}, the peak of HNO radical production rate in reaction (R246) NH_2+O=HNO + H first rises, and then begins to decline when X_{NH3} is greater than .6. Figure 11 shows the effect of X_{NH3} on NO production rate under high temperature and high pressure; Figure 11B shows that with the increase of X_{NH3}, the peak of NO production rate in the reaction (R274) HNO + OH<=>NO + H_2O didn't increase continuously, but

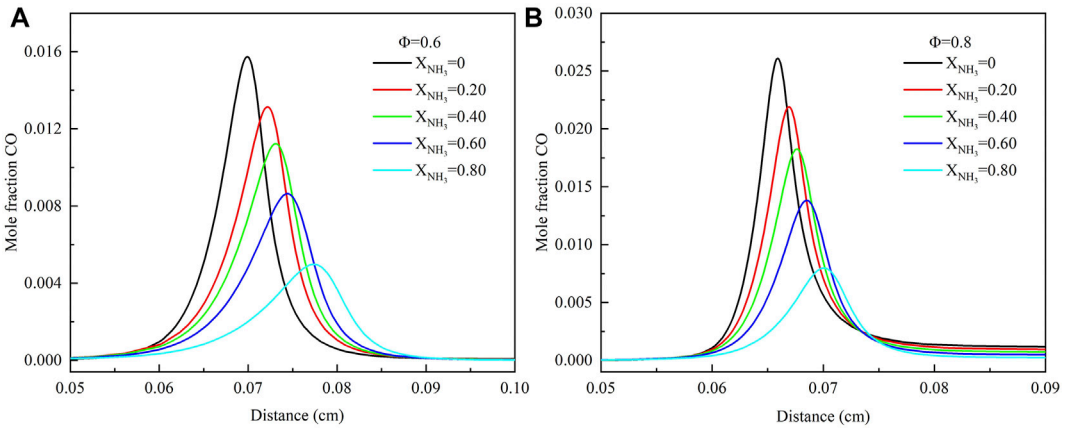

FIGURE 13
Mole fraction of CO with different ammonia content: **(A)** Φ = .6; **(B)** Φ = .8. (T = 723 K, p = 16.5 atm).

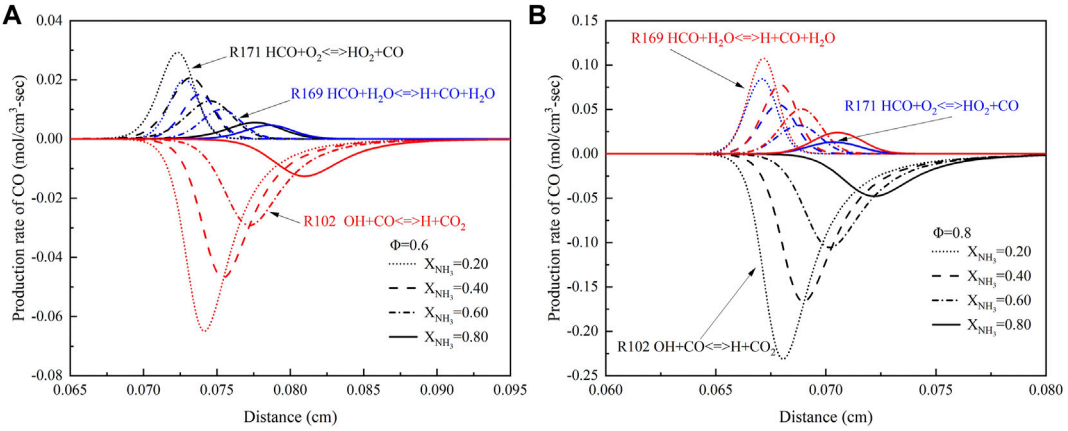

FIGURE 14
The production rate of CO with different ammonia content: **(A)** Φ = .6; **(B)** Φ = .8. (T = 723 K, p = 16.5 atm).

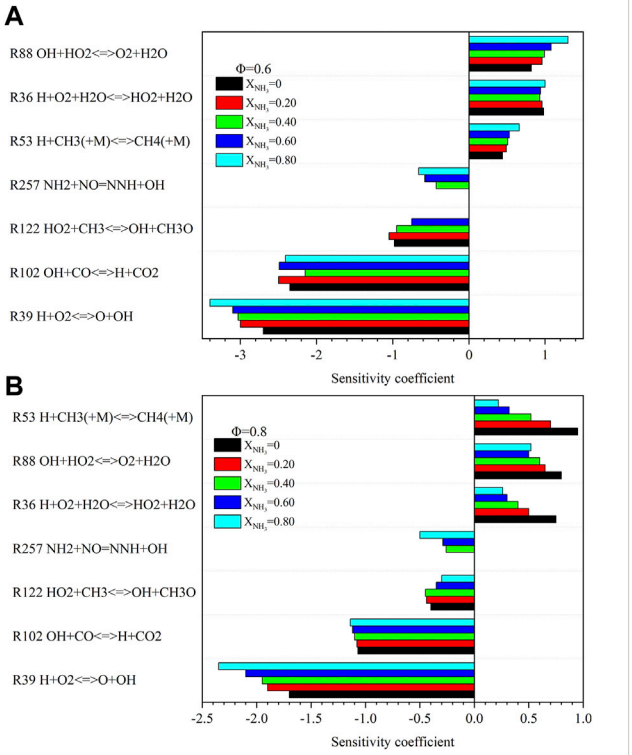

FIGURE 15
Sensitivity analysis of CO with different ammonia content: **(A)** Φ = .6; **(B)** Φ = .8. (T = 723 K, p = 16.5 atm).

reached the maximum at X_{NH3} = .6, and then began to decline. The reason for this trend is that in areas with high ammonia content, the combination of amine radicals with NO leads to a decay of the pollutant (Okafor et al., 2019).

In addition, Figure 11 also shows that the main reactions for NO formation are (R271) H + NO + M<=>HNO + M and (R274) HNO + OH<=>NO + H_2O. With the increase of pressure, the three-body chain termination reaction was enhanced, and the main reaction of NO formation HNO + H<=>H_2+NO was replaced by (R274) at atmospheric pressure. The most important reaction for NO reduction is (R240)NH + NO = N_2O + H. As a direct reaction of NO formation, (R271) generates NO through the consumption of HNO radicals, while (R240) consumes NO through the reaction of NH radicals with NO. The addition of ammonia gas promoted the formation of NH_2 radicals, which resulted in a marked increase in the production rate of (R271) and (R240). In addition, increasing the equivalence ratio can increase the combustion rate, resulting in a shift of the peak position of the NO generation rate towards the flame front.

Figure 12 shows the sensitivity coefficients of NO for different equivalence ratios at high temperatures and high pressure. The most important reaction that promotes NO formation is (R39) H + O_2≤>O + OH. Regardless of the equivalence ratio, the sensitivity coefficient of the reaction (R39) gradually increased with the increase of X_{NH3}. A previous study at room temperature and pressure showed that the reaction (R257) NH_2+NO = NNH + OH is one of the most important reactions to control the NO concentration in the flame of an ammonia/methane mixture (Okafor et al., 2018). However, under high temperature and high pressure environments, reaction (R257) becomes the reaction that promotes NO formation. At Φ = .6, the most important reaction promoting NO reduction is OH + HO_2<=>O_2+H_2O (R88), which is the same as at Φ = .8.

3.6 Effect of ammonia addition on CO formation

Figure 13 shows the effect of the equivalent ratio and X_{NH3} on CO emission at high temperatures and pressure. The results show that the final CO emission slightly increases with the increase of the equivalence ratio (Φ = .6–.8). However, the peak CO mole fraction increased significantly in the combustion reaction. This phenomenon is the same as the change of CO emission with an equivalence ratio at normal temperature and pressure (Xiao et al., 2017b). In order to facilitate the practical application of ammonia/methane mixture fuels, it is preferable to burn in a lean state. This is because the CO emissions are extremely low regardless of the X_{NH3} in the equivalent ratio range of .6–.8. Furthermore, as X_{NH3} increases from 0 to .8, the peak mole fraction of CO is observed to move towards the downstream region of the flame and gradually decrease. The increase of X_{NH3} leads to

decreased carbon element and temperature, so the peak mole fraction of CO is continuously decreasing.

To investigate the effect of ammonia content on CO formation, Figure 14 shows the CO production rate at high temperatures and high pressure. As can be seen from the Figure 14, the main reactions of CO formation are (R171) HCO + O_2<=>HO_2+CO and (R169) HCO + H_2O<=>H + CO + H_2O. These reactions demonstrate that HCO is an important intermediate in CO formation. At high temperatures and pressure, the most important reaction for CO consumption is (R102) OH + CO<=>H + CO_2, and this is true at any equivalence ratio. In addition, both the generation rate and consumption rate of CO decrease with the increase of X_{NH3}. This is because H, O, and OH radicals decrease, and the temperature decreases as the X_{NH3} increases.

Figure 15 shows the effect of X_{NH3} on the sensitivity coefficient of CO at Φ = .6 and .8 under high temperature and high pressure. At Φ = .6, the most critical reaction promoting CO formation is (R88) OH + HO_2<=>O_2+H_2O. The O_2 and H_2O produced by this reaction are necessary to generate CO. When Φ = .8, the most important reaction to promote the formation of CO is (R53) H + CH_3(+M)<=>CH_4(+M), which is different from the important reaction to promote the formation of CO at normal temperature and pressure (Rocha et al., 2019). The sensitivity coefficient of this reaction decreased with the increase of X_{NH3}. Furthermore, the most important reaction to prevent CO formation is (R39) H + O_2 = O + OH. This reaction consumes a lot of O_2.

4 Conclusion

In this paper, the combustion characteristics and NO and CO emissions of different X_{NH3} ammonia/methane fuel blends under gas turbine operating conditions (T = 723 K, p = 16.5 atm) were simulated by Chemkin Pro/Premix Code with Okafor chemical reaction mechanism. The main conclusions are summarized as follows:

(1) The emission of NO is more sensitive to pressure than that of CO. In order to reduce the emission of NO, the pressure can be appropriately increased. In order to solve the problem of excessive emission of the main pollutants, when the ammonia and methane mixed fuel is burned under the condition of an F-class gas turbine, it is better to carry out under the condition of .6 < Φ < .8. Considering carbon emission, the ammonia content can be appropriately increased because the change of ammonia content in the range of .6 < Φ < .8 has little impact on the total pollutant emission.

(2) The flame structure analysis showed that with the increase of X_{NH3} (X_{NH3} = −1.0), the peak molar fraction and production rate of H, O, and OH radical decreased gradually. When the equivalent ratio is .8, the peak molar fraction of H radical is reduced by 76%, O by 82%, and OH by 47%. However, with the increase of X_{NH3} (X_{NH3} = .2–1.0), the peak molar fraction of NH_2 increased by 78%. The main reactions for the formation of H, O and OH radicals are OH + H_2<=>H + H_2O, H + O_2<=>O + OH and 2OH<=>O + H_2O. The main reaction for the formation of NH_2 radicals is NH_3 + OH = NH_2 + H_2O. In addition, the addition of ammonia promotes the decrease of flame temperature and lowers the temperature gradient across the flame region. As the most important reaction promoting the temperature rise, the temperature sensitivity coefficient of H + O_2<=>O + OH decreases with the increase of X_{NH3}.

(3) NO emissions don't increase consistently with the increase of X_{NH3}. When X_{NH3} is greater than .6, NO emission decreases with the increase of X_{NH3}. This trend is the same as at normal temperature and pressure. The most important reaction for NO formation at high temperature and pressure (T = 723 K and p = 16.5 atm) is H + NO + M<=>HNO + M. The most important reaction leading to CO consumption is OH + CO<=>H + CO_2.

Data availability statement

The original contributions presented in the study are included in the article/Supplementary Material, further inquiries can be directed to the corresponding author.

Author contributions

YZ, DZ, and MH carried out the concept, design, knowledge content definition, literature search, data collection, data analysis, and manuscript writing. QL, QH, and JD assisted in data collection, data analysis and statistical analysis. YS, ZM, and JW conducted literature search, data collection and manuscript editing. YZ and MH reviewed manuscripts. All authors have read and accepted the manuscript.

Funding

The project was supported by "20 Policies about Colleges in Jinan" Program (Grant NO: 2019GXRC047) and "migratory bird like" high level talent program in Tianqiao District.

Conflict of interest

JD was employed by Shandong Torch Creation Energy Science and Technology Co., Ltd.

The remaining authors declare that the research was conducted in the absence of any commercial or financial relationships that could be construed as a potential conflict of interest.

Publisher's note

Supplementary material

The Supplementary Material for this article can be found online at: https://www.frontiersin.org/articles/10.3389/fenrg.2023.1120108/full#supplementary-material

References

An, Z., Zhang, M., Zhang, W., Mao, R., Wei, X., Wang, J., et al. (2021). Emission prediction and analysis on CH_4/NH_3/air swirl flames with LES-FGM method. *Fuel* 304, 121370. doi:10.1016/j.fuel.2021.121370

Berwal, P., Kumar, S., and Khandelwal, B. (2021). A comprehensive review on synthesis, chemical kinetics, and practical application of ammonia as future fuel for combustion. *J. Energy Inst.* 99, 273–298. doi:10.1016/j.joei.2021.10.001

Berwal, P., Shawnam and Kumar, S. (2023). Laminar burning velocity measurement of $CH_4/H_2/NH_3$-air premixed flames at high mixture temperatures. *Fuel* 331 (P1), 125809. doi:10.1016/j.fuel.2022.125809

Chen, Y., Zhang, B., Su, Y., Sui, C., and Zhang, J. (2022). Effect and mechanism of combustion enhancement and emission reduction for non-premixed pure ammonia combustion based on fuel preheating. *Fuel* 308, 122017. doi:10.1016/j.fuel.2021.122017

Cheng, M., Wang, H., Xiao, H., Luo, K., and Fan, J. (2021). Emission characteristics and heat release rate surrogates for ammonia premixed laminar flames. *Int. J. Hydrogen Energy.* 46, 13461–13470. doi:10.1016/j.ijhydene.2021.01.154

Collis, J., and Schomäcker, R. (2022). Determining the production and transport cost for H_2 on a global scale. *Front. Energy Res.* 10, 909298. doi:10.3389/fenrg.2022.909298

Colson, S., Kuhni, M., Hayakawa, A., Kobayashi, H., Galizzi, C., and Escudié, D. (2021). Stabilization mechanisms of an ammonia/methane non-premixed jet flame up to liftoff. *Combust. Flame.* 234, 111657. doi:10.1016/j.combustflame.2021.111657

Glarborg, P., Miller, J. A., Ruscic, B., and Klippenstein, S. J. (2018). Modeling nitrogen chemistry in combustion. *Prog. Energy Combust. Sci.* 67, 31–68. doi:10.1016/j.pecs.2018.01.002

Han, X., Wang, Z., Costa, M., Sun, Z., He, Y., and Cen, z. K. (2019). Experimental and kinetic modeling study of laminar burning velocities of NH_3/air, NH_3/H_2/air, NH_3/CO/air and NH_3/CH_4/air premixed flames. *Combust. Flame* 206, 214–226. doi:10.1016/j.combustflame.2019.05.003

He, J., Ying, Y., Chen, M., and Liu, D. (2022). Soot formation characteristics in hybrid pyrolysis of zero-carbon fuel ammonia and ethylene mixtures. *Front. Energy Res.* 10, 996813. doi:10.3389/fenrg.2022.996813

Hu, E., Li, X., Meng, X., Chen, Y., Cheng, Y., Xie, Y., et al. (2015). Laminar flame speeds and ignition delay times of methane-air mixtures at elevated temperatures and pressures. *Fuel* 158, 1–10. doi:10.1016/j.fuel.2015.05.010

Jójka, J., and Ślefarski, R. (2018). Dimensionally reduced modeling of nitric oxide formation for premixed methane-air flames with ammonia content. *Fuel* 217, 98–105. doi:10.1016/j.fuel.2017.12.070

Kanoshima, R., Hayakawa, A., Kudo, T., Okafor, E. C., Colson, S., Ichikawa, A., et al. (2022). Effects of initial mixture temperature and pressure on laminar burning velocity and Markstein length of ammonia/air premixed laminar flames. *Fuel* 310, 122149. doi:10.1016/j.fuel.2021.122149

Khateeb, A. A., Guiberti, T. F., Wang, G., Boyette, W. R., Younes, M., Jamal, A., et al. (2021). Stability limits and NO emissions of premixed swirl ammonia-air flames enriched with hydrogen or methane at elevated pressures. *Int. J. Hydrogen Energy* 46 (21), 11969–11981. doi:10.1016/j.ijhydene.2021.01.036

Khateeb, A. A., Guiberti, T. F., Zhu, X., Younes, M., Jamal, A., and Roberts, W. L. (2020). Stability limits and exhaust NO performances of ammonia-methane-air swirl flames. *Exp. Therm. Fluid Sci.* 114, 110058. doi:10.1016/j.expthermflusci.2020.110058

Kobayashi, H., Hayakawa, A., Somarathne, K. D. K. A., and Okafor, E. C. (2019). Science and technology of ammonia combustion. *Proc. Combust. Inst.* 37 (1), 109–133. doi:10.1016/j.proci.2018.09.029

Kovaleva, M., Hayakawa, A., Colson, S., Okafor, E. C., Kudo, T., Valera-Medina, A., et al. (2022). Numerical and experimental study of product gas characteristics in premixed ammonia/methane/air laminar flames stabilised in a stagnation flow. *Fuel Commun.* 10, 100054. doi:10.1016/j.jfueco.2022.100054

Ku, J. W., Ahn, Y. J., Kim, H. K., Kim, Y. H., and Kwon, O. C. (2020). Propagation and emissions of premixed methane-ammonia/air flames. *Energy* 201, 117632. doi:10.1016/j.energy.2020.117632

Kurata, O., Iki, N., Matsunuma, T., Inoue, T., Tsujimura, T., Furutani, H., et al. (2017). Performances and emission characteristics of NH_3-air and NH_3-CH_4-air combustion gas-turbine power generations. *Proc. Combust. Inst.* 36 (3), 3351–3359. doi:10.1016/j.proci.2016.07.088

Michailos, S., and Gibbins, J. (2022). A modelling study of post-combustion capture plant process conditions to facilitate 95–99% CO_2 capture levels from gas turbine flue gases. *Front. Energy Res.* 10, 866838. doi:10.3389/fenrg.2022.866838

Mikulčić, H., Baleta, J., Wang, X., Wang, J., Qi, F., and Wang, F. (2021). Numerical simulation of ammonia/methane/air combustion using reduced chemical kinetics models. *Int. J. Hydrogen Energy* 46 (45), 23548–23563. doi:10.1016/j.ijhydene.2021.01.109

Nozari, H., and Karabeyoğlu, A. (2015). Numerical study of combustion characteristics of ammonia as a renewable fuel and establishment of reduced reaction mechanisms. *Fuel* 159, 223–233. doi:10.1016/j.fuel.2015.06.075

Okafor, E. C., Naito, Y., Colson, S., Ichikawa, A., Kudo, T., Hayakawa, A., et al. (2018). Experimental and numerical study of the laminar burning velocity of CH_4–NH_3–air premixed flames. *Combust. Flame.* 187, 185–198. doi:10.1016/j.combustflame.2017.09.002

Okafor, E. C., Naito, Y., Colson, S., Ichikawa, A., Kudo, T., Hayakawa, A., et al. (2019). Measurement and modelling of the laminar burning velocity of methane-ammonia-air flames at high pressures using a reduced reaction mechanism. *Combust. Flame.* 204, 162–175. doi:10.1016/j.combustflame.2019.03.008

Okafor, E. C., Somarathne, K. D. K. A., Ratthanan, R., Hayakawa, A., Kudo, T., Kurata, O., et al. (2020). Control of NOx and other emissions in micro gas turbine combustors fuelled with mixtures of methane and ammonia. *Combust. Flame.* 211, 406–416. doi:10.1016/j.combustflame.2019.10.012

Ren, F., Chu, H., Xiang, L., Han, W., and Gu, M. (2019). Effect of hydrogen addition on the laminar premixed combustion characteristics the main components of natural gas. *J. Energy Inst.* 92 (4), 1178–1190. doi:10.1016/j.joei.2018.05.011

Rocha, R. C., Ramos, C. F., Costa, M., and Bai, X. S. (2019). Combustion of NH_3/CH_4/Air and NH_3/H_2/air mixtures in a porous burner: Experiments and kinetic modeling. *Energy fuels.* 33 (12), 12767–12780. doi:10.1021/acs.energyfuels.9b02948

Shi, G., Li, P., Hu, F., and Liu, Z. (2022). NO mechanisms of syngas MILD combustion diluted with N_2, CO_2, and H_2O. *Int. J. Hydrogen Energy* 47 (37), 16649–16664. doi:10.1016/j.ijhydene.2022.03.123

Song, Y., Hashemi, H., Christensen, J. M., Zou, C., Marshall, P., and Glarborg, P. (2016). Ammonia oxidation at high pressure and intermediate temperatures. *Fuel* 181, 358–365. doi:10.1016/j.fuel.2016.04.100

Sun, J., Yang, Q., Zhao, N., Chen, M., and Zheng, H. (2022). Numerically study of CH_4/NH_3 combustion characteristics in an industrial gas turbine combustor based on a reduced mechanism. *Fuel* 327, 124897. doi:10.1016/j.fuel.2022.124897

Sun, Y., Zhang, Y., Huang, M., Li, Q., Wang, W., Zhao, D., et al. (2022). Effect of hydrogen addition on the combustion and emission characteristics of methane under gas turbine relevant operating condition. *Fuel* 324, 124707. doi:10.1016/j.fuel.2022.124707

Valera-Medina, A., Marsh, R., Runyon, J., Pugh, D., Beasley, P., Hughes, T., et al. (2017). Ammonia–methane combustion in tangential swirl burners for gas turbine power generation. *Appl. Energy* 185, 1362–1371. doi:10.1016/j.apenergy.2016.02.073

Valera-Medina, A., Morris, S., Runyon, J., Pugh, D. G., Marsh, R., Beasley, P., et al. (2015). Ammonia, methane and hydrogen for gas turbines. *Energy Procedia* 75, 118–123. doi:10.1016/j.egypro.2015.07.205

Valera-Medina, A., Xiao, H., Owen-Jones, M., David, W. I. F., and Bowen, P. J. (2018). Ammonia for power. *Prog. Energy Combust. Sci.* 69, 63–102. doi:10.1016/j.pecs.2018.07.001

Varghese, R. J., Kolekar, H., Kishore, V. R., and Kumar, S. (2019). Measurement of laminar burning velocities of methane-air mixtures simultaneously at elevated pressures and elevated temperatures. *Fuel* 257, 116120. doi:10.1016/j.fuel.2019.116120

Xiao, H., Howard, M. S., Valera-Medina, A., Dooley, S., and Bowen, P. (2017a). Reduced chemical mechanisms for ammonia/methane Co-firing for gas turbine applications. *Energy Procedia* 105, 1483–1488. doi:10.1016/j.egypro.2017.03.441

Xiao, H., Lai, S., Valera-Medina, A., Li, J., Liu, J., and Fu, H. (2020). Study on counterflow premixed flames using high concentration ammonia mixed with methane. *Fuel* 275, 117902. doi:10.1016/j.fuel.2020.117902

Xiao, H., Valera-Medina, A., and Bowen, P. J. (2017b). Study on premixed combustion characteristics of co-firing ammonia/methane fuels. *Energy* 140, 125–135. doi:10.1016/j.energy.2017.08.077

Zamfirescu, C., and Dincer, I. (2008). Using ammonia as a sustainable fuel. *J. Power Sources* 185 (1), 459–465. doi:10.1016/j.jpowsour.2008.02.097

Zhang, J., Mei, B., Li, W., Fang, J., Zhang, Y., Cao, C., et al. (2022). Unraveling pressure effects in laminar flame propagation of ammonia: A comparative study with hydrogen, methane, and ammonia/hydrogen. *Energy fuels.* 36 (15), 8528–8537. doi:10.1021/acs.energyfuels.2c01766